CELL CYCLE
2020, VOL. 19, NO. 23, 3260–3276
https://doi.org/10.1080/15384101.2020.1839697

Taylor & Francis
Taylor & Francis Group

RESEARCH PAPER

microRNA-877 contributes to decreased non-small cell lung cancer cell growth via the PI3K/AKT pathway by targeting tartrate resistant acid phosphatase 5 activity

Xue Bai#, Changjun He#, Bicheng Fu, Xianglong Kong, Jianlong Bu, Kaibin Zhu, Wei Zheng, Fucheng Zhou, Boxiong Ni, and Shidong Xu

Department of Thoracic, Harbin Medical University Cancer Hospital, Haerbin, Heilongjiang, P.R. China

ABSTRACT

Non-small cell lung cancer (NSCLC) is a leading cause of cancer death in both men and women. microRNAs (miRs) can exert important functions in cancer development. However, the role of miR-877 in NSCLC as it relates to tartrate resistant acid phosphatase 5 (ACP5) is unknown. For this study, the gain-and-loss-of-function experiments were performed to explore the effects of miR-877 and ACP5 on NSCLC. miR-877 expression in LC and paracancerous tissues, lung epithelial cell line and NSCLC cell lines was detected, and the association between miR-877 expression and clinical features of LC patients was analyzed. The levels of ACP5, epithelial-mesenchymal transition (EMT) markers and apoptosis-related proteins were measured. *In vivo* experiments were conducted for further validation. Consequently, we found that miR-877 expression was lowered in LC tissues and cell lines, and correlated with clinical stage, differentiation, lymph node metastasis and prognosis of NSCLC patients. Additionally, miR-877 was determined to inhibit ACP5 activity, and miR-877 downregulated the PI3K/AKT pathway by silencing ACP5. Furthermore, overexpression of miR-877 inhibited the viability, migration, invasion and EMT of NSCLC cells, but promoted cell apoptosis. In conclusion, miR-877 overexpression inhibited malignant biological behaviors of NSCLC cells by downregulating ACP5 and inactivating the PI3K/AKT pathway.

ARTICLE HISTORY
Received 22 November 2019
Revised 19 July 2020
Accepted 15 October 2020

KEYWORDS
Non-small cell lung cancer; microRNA-877; tartrate resistant acid phosphatase 5; PI3K/AKT pathway

Introduction

Lung cancer (LC) has long been regarded as the most concerning malignancy worldwide as it causes the highest morbidity among men and the second highest among women [1]. At present, approximately 70% of LC patients are diagnosed at advanced stages because of the lack of early-stage symptoms, and unfortunately, the five-year survival rate is only 16% [2]. Non-small cell lung cancer (NSCLC) accounts for 85% of the cases of lung cancer, and 70% of NSCLC patients have locally advanced or metastatic disease at the time of diagnosis, with 15% to 20% 5-year overall survival rate [3]. Smoking has been identified as the major cause of LC, which is responsible for over 80% of cases, and notably, the incidence has started to decline with severe tobacco control implementations [4]. Additionally, air pollution and residential radon are increasingly recognized as the risk factors for LC [5,6]. Novel treatment methods based on molecular pathways, mainly the epidermal growth factor receptor, anaplastic lymphoma kinase, and serine/threonine-protein kinase B-Raf, are now as emerging approaches for LC treatment [7]. Recently, substantial progress made in the understanding of the molecular events essential for tumor initiation and progression has accelerated the development of molecular-targeted regimens for cancers, which are widely recognized as valuable therapeutic treatments for NSCLC [8]. Therefore, finding novel biomarkers for the early diagnosis and effective treatment of NSCLC based on molecular-targeted regimens has become increasingly important.

microRNAs (miRs), a group of small non-coding RNA molecules, have important effects on cell differentiation, proliferation and apoptosis, and their imbalance causes tumor progression, including LC [9]. A member of miRs, miR-877

CONTACT Changjun He he_changjun_cool@126.com; Shidong Xu drxushidong123@163.com

#These authors are contributed equally to this paper

has been previously reported as a tumor suppressor in renal cell carcinoma (RCC) [10], and miR-877-3p could suppress myofibroblast differentiation of lung resident mesenchymal stem cells and alleviate lung fibrosis [11]. However, the mechanism of miR-877 in LC cells has not been elucidated thus far. In our study, using a dual-luciferase reporter gene assay, we found that miR-877 targeted tartrate resistant acid phosphatase 5 (ACP5) and inhibited ACP5 expression. ACP5, also known as tartrate-resistant acid phosphatase (TRAP), is derived from osteoclasts, osteoblasts and osteocytes, and inactivating mutations in ACP5 contribute to spondyloenchondrodysplasia, which involves autoimmunity disease characteristics [12]. Interestingly, high ACP5 expression is associated with tumor development and serves as an underlying prognostic marker for lung adenocarcinoma [13]. The phosphatidylinositol-3 kinase (PI3K)/protein kinase B (AKT) pathway is activated in 90% of non-small cell lung cancer (NSCLC) cells and its inhibition is pivotal for finding new approaches for NSCLC treatment [14]. Based on the above observations, we hypothesized that miR-877 and ACP5 might cooperate in NSCLC progression. Thus, we conducted a study to investigate how miR-877 acts on NSCLC by regulating ACP5 to find a new clinical reference for NSCLC patients.

Materials and methods

Ethics statement

This study was approved and supervised by the ethics committee of the Harbin Medical University Cancer Hospital. All the subjects signed the informed consent. The protocol was also approved by the Institutional Animal Care and Use Committee of the Harbin Medical University Cancer Hospital. Significant efforts were made to minimize both the number of animals used and their respective suffering.

Sample collection

From September 2012 to June 2013, 80 resected LC tissues and paracancerous tissues (over 5 cm away from cancer tissues) from LC patients (57 males and 23 females, median age: 49 ~ 79 years, average age: 64.9 ± 7.3 years) who were diagnosed and treated at the Harbin Medical University Cancer Hospital were enrolled in this experiment. All patients were followed up every three months for five years. Patients were enrolled in this study if they met the following criteria: 1) patients who were diagnosed with LC by the detection of various indicators; 2) patients who had not received radiotherapy or chemotherapy; and 3) patients who had complete clinical data. Patients complicated with chronic system diseases or other malignant tumors were excluded.

Cell culture

Human NSCLC cell lines H1299, 95 C, A549, SPC-A-1 and L9981, and lung epithelial cells BEAS-2B (Cancer Cell Bank of Chinese Academy of Medical Sciences, Beijing, China) were cultured at 1×10^5 cells/cm^2 respectively in Roswell Park Memorial Institute (RPMI)-1640 medium containing 10% fetal bovine serum (FBS) (Gibco Company, Grand Island, NY, USA) for 48 hours (37°C, 5% CO_2). When cell confluence reached 80% ~ 90%, cells were detached with 0.025% trypsin (Gibco Company, Grand Island, NY, USA) and passaged.

Cell transfection

Cultured SPC-A-1 cells were transfected with phosphate buffer saline (PBS), miR-negative control (NC), or miR-877 mimic, and named as blank group, miR-NC group and miR-877 group, respectively. Then, an ACP5 overexpression plasmid was constructed and transfected into cells from the miR-877 group, which was named the overexpression (OE) group. The 95 C cells were transfected with PBS, miR-NC or miR-877 inhibitor (GenePharma, Shanghai, China), and were named blank group, miR-NC group and miR-IN group, respectively. All operations were performed according to the instructions of the Lipofectamine^{TM} 3000 kit (Invitrogen, Carlsbad, CA, USA).

Dual luciferase reporter gene assay

The online prediction software miRWalk (http://mirwalk.umm.uni-heidelberg.de/) was employed to predict the binding site between miR-877 and the 3'-untranslated region (3'UTR) of ACP5. ACP5 wild-type (WT) and coding sequence CDS-binding mutant (MT) were synthesized by Sangon Biotech (Shanghai) Co., Ltd. (Shanghai, China) and inserted into pMIR-REPORT™ (Thermo Fisher Science, Carlsbad, California, USA) luciferase reporter vector. Lipofectamine 3000 transfection kit (Invitrogen Inc., Carlsbad, California, USA) was used to co-transfect WT plasmid, MT plasmid, miR-877 mimic and miR-NC into 293 T cells. After 24 hours, the cells were lysed and luciferase activity was detected using a Dual-Luciferase Reporter Assay System (Promega Corporation, Madison, Wisconsin, USA).

Quantitative real-time polymerase chain reaction (qRT-PCR)

Total RNA from LC tissues and cells was obtained using the RNAiso Plus (Takara, Otsu, Shiga, Japan) and Trizol LS Reagent (Takara, Otsu, Shiga, Japan) separately. Then formaldehyde denaturation electrophoresis was used to verify the reliability of the obtained RNA, and subsequent experiments were performed. Reverse transcription (RT)-PCR was conducted according to the manufacturer's protocol using PrimeScript™ RT reagent kit (Takara, Otsu, Shiga, Japan). The mRNA expression was quantified by standard RT-PCR protocol with SYBR Premix Ex Taq (Takara, Otsu, Shiga, Japan). U6 and glyceraldehyde-3-phosphate dehydrogenase (GAPDH) was used references and the primers are shown in Table 1.

Western blot analysis

Total protein was extracted by radioimmunoprecipitation assay lysis buffer containing phenylmethylsulfonyl fluoride (Beyotime Biotechnology Co., Ltd, Shanghai, China) and the protein level in the supernatant was determined by the bicinchoninic acid (BCA) method. An equal volume (50 μg) of protein was separated by 10% sodium dodecyl sulfate polyacrylamide gel electrophoresis, and then transferred into the polyvinylidene fluoride membrane (Millipore Corp, Billerica, MA, USA). The PVDF membrane was then incubated with Tris-buffered saline Tween (TBST) (Boster Biological Technology Co., Ltd, Wuhan, Hubei, China) containing 5% skimmed milk at room temperature to block nonspecific binding. Subsequently, the membrane was cultured with primary antibodies (all from Abcam Inc., Cambridge, MA, USA) (Table 2) at 4°C overnight, and then with rabbit anti-rat secondary antibody at room temperature for 1 hour. The proteins were colored by enhanced chemiluminescence reagent, and visualized using a BioSpectrum gel imaging system (Bio-Rad, Hercules, CA, USA).

Table 1. Primer sequences of qRT-PCR.

Primers	Sequences
miR-877	F: TCACACTATATCACATTGCCAGG
	R: TATGGTTGTTCTGCTCTCTGTCTC
U6	F: GACGAATGGAAGAGCCTGAC
	R: ACGCTTCACGAATTTGCGTGTC
ACP5	F: AGATCCTGGGTGCAGACTTC
	R: GTAGAAAGGGCTGGGGAAG
E-cadherin	F: TCACATCCTACACTGCCCAG
	R: AGTGTCCCTGTTCCAGTAGC
N-cadherin	F: AGGGGACCTTTTCCTCAAGA
	R: TCAAATGAAACCGGGCTATC
GAPDH	F: ACAGTCAGCCGCATCTTCTT
	R: GACAAGCTTCCCGTTCTCAG

qRT-PCR, Quantitative real-time polymerase chain reaction; miR-877, microRNA-877; ACP5, tartrate resistant tartrate resistant acid phosphatase 5; GAPDH, glyceraldehyde-3-phosphate dehydrogenase; F, forward; R, reverse.

Table 2. Antibodies used for western blot analysis.

Antibodies	No.	Dilution ratio
ACP5	ab37150	1: 500
Bcl-2	ab32124	1: 1000
E-cadherin	ab1416	1:50
N- cadherin	ab18203	1: 100
Cleaved caspase-3	ab2302	1:50
Cleaved PARP	ab32064	1: 5000
PI3K	ab76234	1: 1000
AKT	ab8805	1: 500
β-actin	ab179467	1: 5000

ACP5, tartrate resistant tartrate resistant acid phosphatase 5; Bcl-2, B-cell lymphoma-2; PARP, poly (ADP-ribose) polymerase; PI3K, phosphatidylinositol-3 kinase; AKT, protein kinase B.

3-(4, 5-dimethylthiazol-2-yl)-2, 5-diphenyltetrazolium bromide (MTT) assay

Cells in logarithmic growth phase were detached by trypsin and resuspended into single cell suspension at 1×10^4 cells/mL. After mixing, the cells were seeded into 96-well plates at 2×10^3 cells/well (equal to 200 μL). Wells were added with culture medium only without cells served as the control. Following inoculation, the cells were cultured in an incubator (37°C, 5% CO_2) for 0 ~ 3 days. After culture for 0 hour, 24 hours, 48 hours and 72 hours, each well was added with 20 μL MTT solution (5 mg/mL), and incubated for additional 4 hours. The supernatant was then removed, 200 μL dimethyl sulfoxide was added to each well, and the solution was vortexed for 10 minutes to fully dissolve the crystals. The optical density (OD) value at a wavelength of 490 was measured using a microplate reader. The experiment was performed three times independently.

Colony formation assay

SPC-A-1 cells at passage 3 in good condition were treated with 0.025% trypsin and then seeded into 6-well plates at 1000 cells/well. After culture at 37°C with 5% CO_2 for 14 days, cells were treated with 75% methanol for 30 minutes, then stained with 0.2% crystal violet to count the number of colonies. Each experiment was repeated 3 times.

5-ethynyl-2 -deoxyuridine (EdU) labeling assay

Cell-light EdU fluorescence detection kit (RiboBio, Guangzhou, Guangdong, China) was applied to measure the DNA replication ability of well-grown cells at passage 3. The cells were treated in line with the instructions of the EdU kit. Under a fluorescence microscope (FSX100, Olympus Optical Co., Ltd, Tokyo, Japan), five visual fields were randomly selected for imaging. Blue fluorescence represented all cells, while red fluorescence represented the replicating cells infiltrated by EdU. The percentage of EdU-positive cells was then calculated.

Immunofluorescence assay

Cells grown on cover glass were washed in PBS 3 times and fixed in 4% polyformaldehyde for 15 minutes at 4°C. After treatment with 0.5% Triton-100 X for 20 minutes, the primary antibodies against E-cadherin and Vimentin-1 were added to the cells to incubate overnight at 4°C. Afterward, the slides were washed in PBS and incubated with fluorescent goat anti-rabbit secondary antibody at 37°C for 1 hour. Finally, cells were observed under a fluorescence microscope (DM3000, Leica, Solms, Germany).

Scratch test

Cell migration ability was measured by cell scratch test. Cells were inoculated into 6-well plates at 5×10^5 cells/well and cultured at 37°C for 24 hours with 5% CO_2. Then a scratch was made on the monolayer cells with a 1 mL pipette tip. Photographs were taken under a microscope at 0 hour and 24 hours to calculate the relative cell migration distance.

Transwell assay

Matrigel (BD Biosciences, Franklin Lakes, NJ, USA) was added into the apical chamber for 30 minutes under sterile conditions. Then the apical chamber was filled with 30 μL RPMI-1640 medium and placed in a CO_2 incubator for reserve. Following detachment, centrifugation, and serum-free resuspension, the cells were diluted into 5×10^5 cells/mL cell suspension. A total of 500 μL RPMI 1640 medium with 10% FBS was placed into the basolateral chamber, and 200 μL cell suspension was added into the apical chamber. Then, the Transwell plate was cultured at 37°C with 5% CO_2 for 48 hours. The chamber was removed, the culture medium was washed with PBS and cells were stained with crystal violet for 10 minutes. Next, crystal violet on the surface of the chamber was washed away with running water, and the non-invading cells on the apical chamber were removed by wiping with cotton swabs. The invading cells were imaged under the microscope to calculate the number of cells.

Flow cytometry

Cultured cells were washed with PBS and detached with 0.025% trypsin and then treated with 70% formaldehyde (v/v) at 20°C for 24 hours. Next, cells were stained with 50 μg/mL propidium iodide (PI) containing 10 μg/mL RNase for 20 minutes. Finally, the cell cycle distribution was measured by using a flow cytometer.

The cell suspensions were mixed with 5 μL Annexin V-fluorescein isothiocyanate (FITC) and 5 μL PI in the dark for 10 minutes. After staining, cell apoptosis was measured by a flow cytometer.

Hoechst 33,258 staining

Cultured cells were fixed with 4% paraformaldehyde for 20 minutes and then stained with Hoechst 33,258 (10 μg/mL) in the dark for 5 minutes. Finally, the cells in five fields in each group were randomly selected for analysis by a fluorescence microscope. The chromatin of apoptotic cells was concentrated and the nuclei were identified as heterogeneous plaque inclusions. Contrary to the normal nuclei, the nuclei of apoptotic cells showed diffuse and homogeneous staining.

Xenograft tumors in nude mice

Thirty specific pathogen-free BALB/c nude mice (4 ~ 6 weeks old, 20 ± 2 g) (Beijing Vital River Laboratory Animal Technology Co., Ltd, Beijing, China, SCXK (Beijing) 2015–0001), were numbered by body weight as a parameter and randomly assigned into six groups, with 5 mice in each group. A total of 4×10^6 SPC-A-1 cells and 95 C cells were administered by saline and injected into the nude mice. Tumor volume was measured every 7 days, mice were euthanized 28 days later, and tumors were removed and weighed for immunohistochemistry. Tumor volume = $M_1^2 \times M_2 \times 0.5236$ [15], in which M_1 represented the shortest axis and M_2 represented the longest axis.

Immunohistochemistry

The extracted cancer tissues of mice were routinely paraffin-embedded and dewaxed. Each tissue sample was sliced into 5 equal sections and cleaned with PBS 3 times and treated with 3% H_2O_2 for 15 minutes at room temperature to eliminate the activity of endogenous peroxidase. After 3 washes with PBS, the sections were incubated with normal goat serum blocking buffer, and kept for 15 minutes at room temperature. After that, the sections were incubated with 50 μL rabbit anti-human Ki67 antibody (1: 500, ab15580, Abcam Inc., Cambridge, MA, USA) at 4°C overnight. After 3 PBS washes, the sections were incubated with secondary antibody at 37°C for 15 minutes. The sections were washed 3 times in PBS, incubated with 40 μL horseradish peroxidase-labeled streptavidin-working solution and incubated at 37°C for 15 minutes. Then the sections were washed with PBS 3 times again, visualized with 2, 4-diaminobutyric acid (DAB), counterstained with hematoxylin for 30 seconds after washing with distilled water, and sealed with neutral gum after dehydration. Five non-overlapping visual fields were selected in each section for observation under the

microscope. The cells with brown-yellow or brown granules in the nucleus were Ki67 positive cells. Five regions were selected at random in each section to count the positive cells expressing Ki67 protein.

Terminal deoxynucleotidyl transferase (TdT)-mediated dUTP nick end labeling (TUNEL) assay

TUNEL assay was employed to detect apoptosis in mouse tumor tissues. TUNEL kit (Roche, Basel, Sweden) was used in the experiment. All procedures were carried out strictly in accordance with the instructions. The stained cells with condensed nuclei were TUNEL-positive cells, namely, apoptotic cells. Five visual fields were randomly selected for observation and counting.

Statistical analysis

SPSS 21.0 (IBM Corp., Armonk, NY, USA) was applied for data analysis. The Kolmogorov-Smirnov test showed whether the data were in normal distribution. The results are presented as the mean ± standard deviation. The t test was employed for analysis of comparisons between two groups, one-way analysis of variance (ANOVA) for comparisons among multi-groups, and Tukey's post hoc test for pairwise comparisons after ANOVA. Fisher's exact test was employed to compare the enumeration data. The p value was obtained by a two-tailed test, and $p < 0.05$ indicated a significant difference.

Results

miR-877 is poorly expressed in LC

According to our previous experimental results, ACP5 was upregulated in LC tissues and promoted LC cell growth, invasion and migration. To further elucidate the upstream molecular mechanism of abnormal expression of ACP5 in LC, the online prediction software TargetScan (http://www.targetscan.org/vert_72/) and miRWalk (http://mirwalk.umm.uni-heidelberg.de/) were applied to predict which miR could target ACP5. After cross-comparison, we found that ACP5 could bind to multiple miRs at 3 UTR region (Figure 1(a)). Subsequently, OncoMir (http://www.oncomir.org/cgi-bin/dbSearch.cgi), an online bioinformatics analysis website, predicted that only miR-877 was associated with LC and was poorly expressed in lung adenocarcinoma tissues, but highly expressed in normal tissues (Figure 1(b)). Furthermore, the dual luciferase reporter gene assay confirmed that ACP5 is a direct target gene of miR-877 (Figure 1(c)).

miR-877 expression in LC tissues was verified by qRT-PCR. The results showed that miR-877 expression in LC tissues was dramatically lower than that in paracancerous tissues ($p < 0.01$, Figure 1(d)), and was negatively correlated with ACP5 expression (Figure 1(e)). In lung epithelial cells BEAS-2B, miR-877 expression was higher than that in NSCLC cells L9981, 95 C, SPC-A-1 and A549 (all $p < 0.05$, Figure 1(f)), indicating that miR-877 was abnormally downregulated in LC tissues. The relative miR-877 expression was the lowest in the SPC-A-1 cell line and highest in the 95 C cell line. Therefore, SPC-A-1 and 95 C cell lines were selected for subsequent experiments.

miR-877 expression is related to clinical stages, differentiation degree, lymph node metastasis and prognosis of LC patients

The relationship between miR-877 expression and the clinical characteristics of LC patients was analyzed. Patients whose relative miR-877 expression was lower than 0.49 (median value) were treated as the low expression group, and the rest were the high expression group. In LC tissues, miR-877 expression was related to clinical stages, lymph node metastasis and tumor differentiation. miR-877 expression decreased with increasing clinical stages of LC patients. miR-877 expression in cancer tissues of patients at stage III + IV, with low differentiation and lymph node metastasis was notably lower than that in patients at stage I + II, with highly differentiation and patients with non-lymph node metastasis (all $p < 0.05$). There was no significant correlation between miR-877 expression and age, gender or tumor size (all $p > 0.05$,

a

Mirna	Refseqid	Genesymbol	Score	Position
hsa-miR-877-3p	XM_005259938	ACP5	1.00	3UTR
hsa-miR-877-3p	NM_001111035	ACP5	1.00	3UTR
hsa-miR-877-3p	NM_001111036	ACP5	1.00	3UTR
hsa-miR-877-3p	NM_001611	ACP5	1.00	3UTR
hsa-miR-133b	NM_001611	ACP5	0.82	3UTR
hsa-miR-532-5p	NM_001611	ACP5	0.82	3UTR
hsa-miR-153-5p	NM_001111035	ACP5	0.82	3UTR
hsa-miR-483-3p	NM_001111035	ACP5	0.85	3UTR
hsa-miR-497-5p	NM_001111035	ACP5	0.85	3UTR

b

miRNA Name	Cancer Abbreviation	T-Test P-value	T-Test FDR	Upregulated in:	Tumor Log2 Mean Expression	Normal Log2 Mean Expression
hsa-miR-877-3p	BRCA	1.16e-03	2.65e-03	Tumor	0.12	0.00
hsa-miR-877-3p	LUAD	3.03e-02	6.89e-02	Normal	0.01	0.34

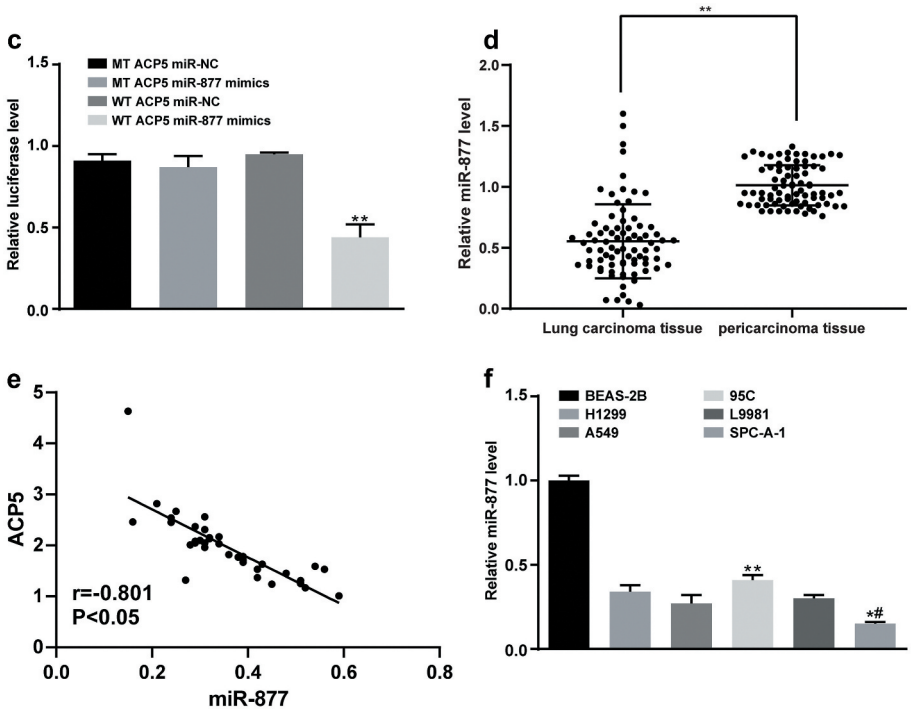

Figure 1. miR-877 is poorly expressed in LC. (a). ACP5 could bind to multiple miRs at the 3 UTR region; (b). miR-877 is downregulated in lung adenocarcinoma tissues, * $p < 0.05$, ** $p < 0.01$; (c). miR-877 binds to ACP5 mRNA and inhibits its activity; (d). miR-877 is downregulated in LC tissues, n = 80; (e). The miR-877 level is negatively correlated to the ACP5 level in LC patients, n = 80; (f). Relative miR-877 expression in L9981, 95 C, H1299, A549, SPC-A-1 and BEAS-2B cell lines, n = 3; All * $p < 0.05$. miR-877, microRNA-877; LC, lung cancer; ACP5, tartrate resistant acid phosphatase 5.

Table 3). Subsequently, Kaplan-Meier survival analysis based on follow-up records revealed that patients with low miR-877 expression had a worse prognosis, showing a 5-year survival rate of 18.9% and an average survival time of 26.8 months after diagnosis; while patients with high miR-877

Table 3. Association between miR-877 expression and clinical stages, differentiation degree and lymph node metastasis of LC patients.

Clinical data	N	miR-877 expression in LC tissues		*P* value
		Low expression (n = 40)	High expression (n = 40)	
Age (years)				0.823
≤ 65	38	18 (45.5)	20 (50.0)	
> 65	42	22 (54.5)	20 (40.0)	
Gender				0.622
Male	57	30 (75.0)	27 (67.5)	
Female	23	10 (25.0)	13 (32.5)	
Tumor diameter (cm)				0.999
≤ 3	33	17 (42.5)	16 (40.0)	
> 3	47	23 (57.5)	24 (60.0)	
Clinical stage				0.012
I + II	34	23 (57.5)	11 (27.5)	
III + IV	46	17 (42.5)	29 (72.5)	
Lymph node metastasis				< 0.001
No	48	13 (32.5)	32 (87.5)	
Yes	32	27 (67.5)	8 (12.5)	
Differentiation				< 0.001
Poor + moderate	52	36 (90.0)	16 (40.0)	
High	28	4 (10.0)	24 (60.0)	

miR-877, microRNA-877; LC, lung cancer.

expression had a relatively better prognosis, with a 5-year survival rate of 37.2% and an average survival time of 36.7 months after diagnosis (all $p < 0.05$, Figure 2).

Overexpression of miR-877 inhibits NSCLC cell growth *in vitro*

Considering that miR-877 expression was related to the clinical stages, differentiation degree and lymph node metastasis of LC patients, nest we explored the effects of miR-877 on the molecular processes of LC. MTT assay was used to measure cell viability and showed no significant difference in cell viability between SPC-A-1 cells in the miR-NC and blank groups in SPC-A-1 cells ($p > 0.05$). Cell viability and proliferation rate in miR-877-overexpressing cells were substantially lower than those in the blank and miR-NC groups at 24 hours, 48 hours and 72 hours; while in 95 C cells, the inhibition of miR-877 increased cell viability and proliferation rate ($p < 0.05$, Figure 3(a)).

The colony formation ability of SPC-A-1 cells was tested with colony formation assay. The results indicated that in SPC-A-1 cells, the number of colonies in miR-877-overexpressing cells decreased significantly as compared with that in the miR-NC group and contrary to those in 95 C cells in the miR-877-IN group (both $p < 0.05$, Figure 3(b)).

EdU assay was used to measure the DNA replication activity of SPC-A-1 cells and showed the DNA replication activity of SPC-A-1 cells was obviously

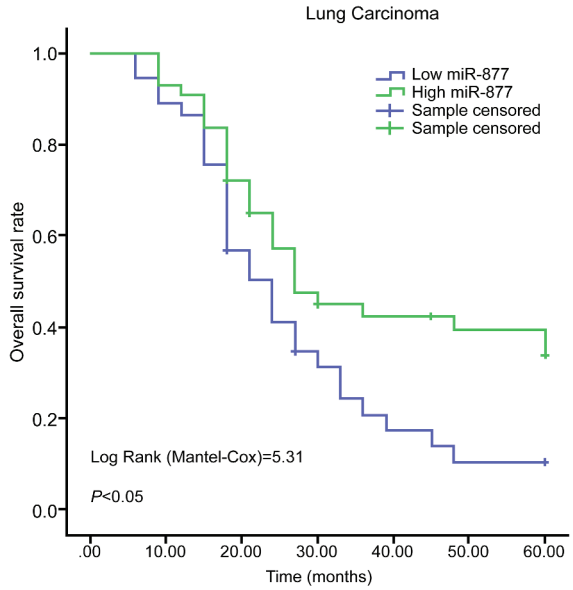

Figure 2. miR-877 expression is related to prognosis of LC patients. miR-877, microRNA-877; LC, lung cancer.

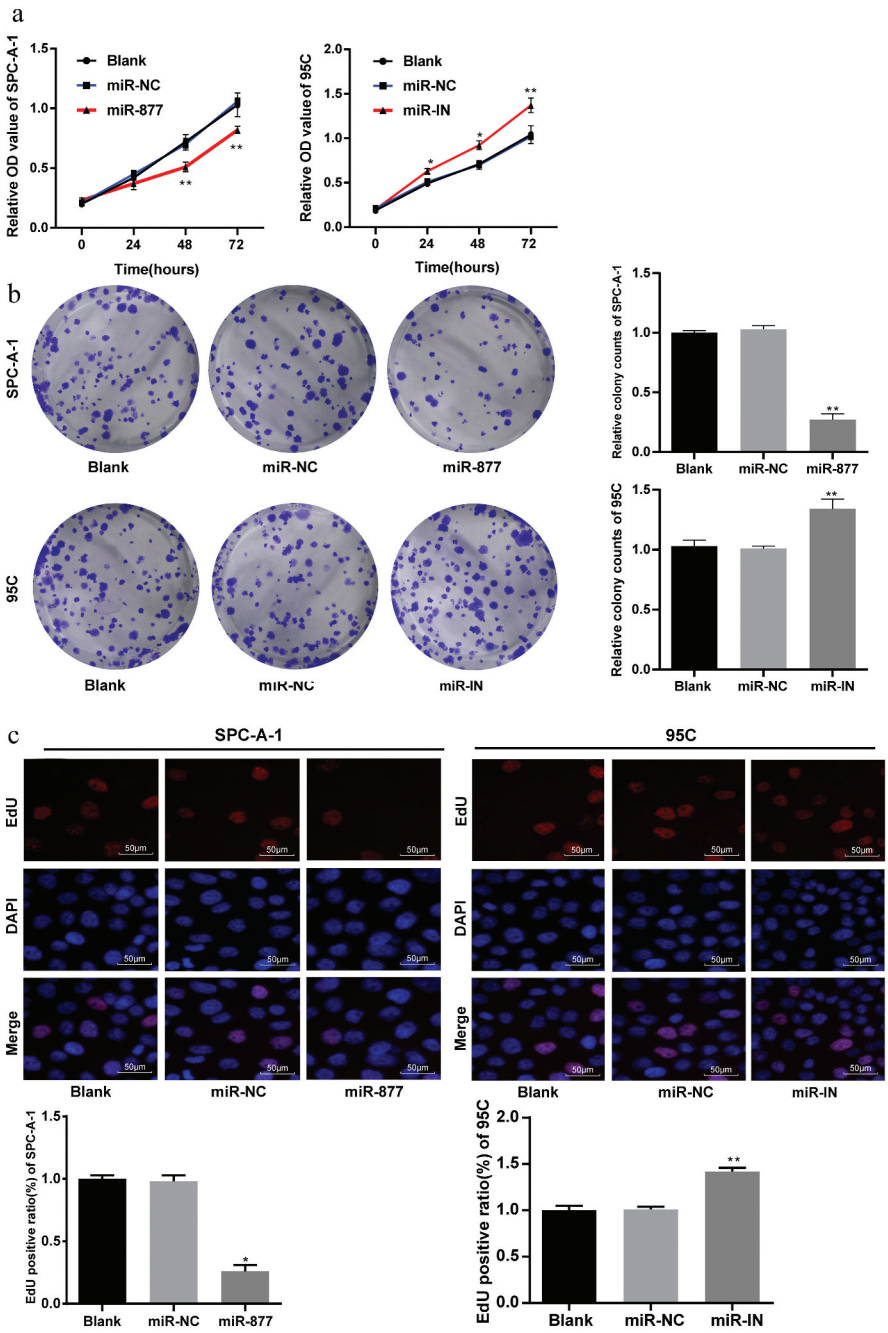

Figure 3. miR-877 overexpression decreases NSCLC cell viability. In the SPC-A-1 cells miR-877 was overexpressed and in the 95 C cells the miR-877 was inhibited. (a). Relative OD value detected using MTT assay; (b). Representative images and statistical chart of relative colony counts detected by colony formation assay; (c). Representative images and statistical chart of EdU-positive cells detected by EdU assay. The experiment was performed three times independently. The results are presented as the mean ± standard deviation. Compared to the miR-NC group, * $p < 0.05$, ** $p < 0.01$. miR-877, microRNA-877; LC, lung cancer; OD, optical density; EdU, 5-ethynyl-2 -deoxyuridine; NC, negative control.

inhibited by overexpression of miR-877, indicating a reduced number of EdU-positive cells. In 95 C cells, inhibition of miR-877 increased the number of EdU-positive cells (all $p < 0.05$, Figure 3(c)).

Overexpression of miR-877 induces apoptosis and cell cycle arrest in NSCLC cells

Flow cytometry was applied to detect the effects of miR-877 on SPC-A-1 and 95 C cell cycle distribution. Compared with those in miR-NC group, cells arrested at G0/G1 and S phase were decreased, cells in G2/M phase were increased in the group with miR-877 overexpression; while cells arrested at S phase increased markedly in the group with inhibited miR-877 expression (all $p < 0.05$, Figure 4(a)). These results suggested that overexpression of miR-877 promoted cell G2/M arrest and inhibited NSCLC cell cycle progression.

Flow cytometry was used to detect the apoptotic rate of SPC-A-1 cells and 95 C cells, and showed that overexpression of miR-877 promoted SPC-A-1 cell apoptosis as compared with cells transfected with miR-NC; while in 95 C cells, inhibition of miR-877 expression resulted in a dramatic decrease in the apoptotic rate (both $p < 0.05$, Figure 4(b)), indicating that overexpression of miR-877 could promote NSCLC cell apoptosis.

Morphological changes of apoptotic cells were observed using Hoechst 33,258 staining and observed under a fluorescence microscope. Compared with the miR-NC group, apoptotic SPC-A-1 cells in cells overexpressing miR-877 were substantially increased; while apoptotic 95 C cells were significantly decreased in the miR-IN group (both $p < 0.05$, Figure 4(c)).

Western blot analysis (Figure 4(d)) revealed that the levels of cleaved caspase-3 and cleaved PARP in SPC-A-1 cells were increased in cells overexpressing miR-877, while Bcl-xl expression was decreased compared with those in the blank and miR-NC groups (all $p < 0.05$). Levels of cleaved caspase-3 and cleaved PARP in 95 C cells were notably decreased in cells with inhibited miR-877 expression, but anti-apoptotic protein Bcl-xl showed the opposite trend (all $p < 0.05$). Combining the above results, we concluded overexpression of miR-877 can promote NSCLC cell apoptosis.

Overexpression of miR-877 inhibits the epithelial-mesenchymal transition (EMT), migration and invasion of NSCLC cells

EMT is a phenotypic change closely related to tumor metastasis. The markers of EMT are E-cadherin decrease and N-cadherin increase. The results of qRT-PCR and western blot analysis suggested that in SPC-A-1 cells, compared with that in the miR-NC group, the E-cadherin level in cells overexpressing miR-877 increased markedly, and the N-cadherin level decreased substantially, which was opposite in 95 C cells with inhibited miR-877 expression (all $p < 0.05$, Figure 5(a,b)). Immunofluorescence assay results showed in SPC-A-1 cells, overexpression of miR-877 increased the number of E-cadherin-positive cells and decreased the number of vimentin-positive cells; while in 95 C cells, inhibition of miR-877 decreased the number of E-cadherin-positive cells and enhanced the number of vimentin-positive cells (all $p < 0.05$, Figure 5(c)).

We further studied the effect of miR-877 on the invasive ability of SPC-A-1 cells and 95 C cells by Transwell assay. The results revealed that the invasive ability of SPC-A-1 cells overexpressing miR-877 was significantly decreased compared to that of the miR-NC group; while the invasive ability of 95 C cells with inhibited miR-877 was significantly increased (both $p < 0.05$, Figure 5(d)).

In vitro migration experiments showed that the migration ability of SPC-A-1 cells was significantly weakened in cells with overexpressed miR-877 when compared with the miR-NC group; while in 95 C cells, inhibiting the expression of miR-877 significantly enhanced cell migration ability (both $p < 0.05$) (Figure 5(e)). Therefore, it can be concluded that overexpression of miR-877 in NSCLC cells can inhibit EMT, while inhibition of miR-877 can promote EMT.

miR-877 represses the growth, invasion and migration of NSCLC cells by decreasing ACP5

Levels of ACP5 in SPC-A-1 cells and 95 C cells were detected using qRT-PCR and Western blot analysis. The results showed that overexpression of miR-877 inhibited ACP5 levels in SPC-A-1 cells, while inhibition of miR-877 increased ACP5 levels (both $p < 0.05$) (Figure 6(a,b)).

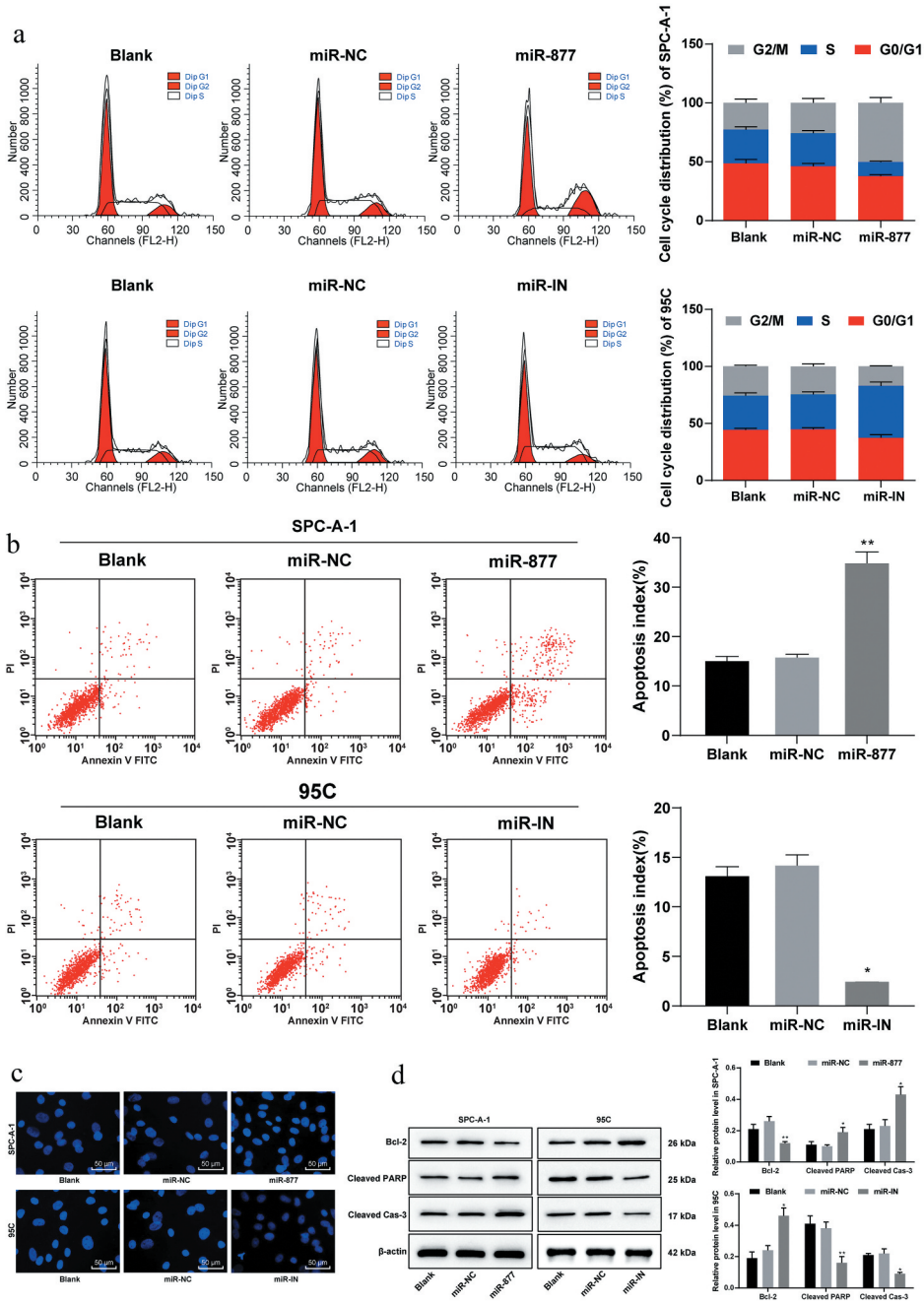

Figure 4. Overexpression of miR-877 promotes NSCLC cell apoptosis and cell cycle arrest. In the SPC-A-1 cells miR-877 was overexpressed and in the 95 C cells the miR-877 was inhibited. (a). Cell cycle distribution of SPC-A-1 cells and 95 C cells by flow cytometry; (b). Apoptosis rate of SPC-A-1 cells and 95 C cells by flow cytometry; (c). Representative images of morphological changes of apoptotic cells by Hoechst 33,258 staining; (d). Relative levels of apoptosis-related markers detected by western blot analysis. The experiment was performed three times independently. The results are presented as the mean ± standard deviation. Compared to the miR-NC group, * $p < 0.05$, ** $p < 0.01$. miR-877, microRNA-877; LC, lung cancer; NC, negative control.

To confirm that miR-877 mainly affects LC cell biological behaviors by regulating ACP5 expression, we constructed an ACP5 overexpression plasmid and, using the Lipofectamine ™ 3000 kit, transfected the ACP5 overexpression plasmid or an empty vector into SPC-A-1 cells overexpressing miR-877, which were called the OE group and NC group, respectively. After 48 hours of transfection, subsequent experiments were carried out.

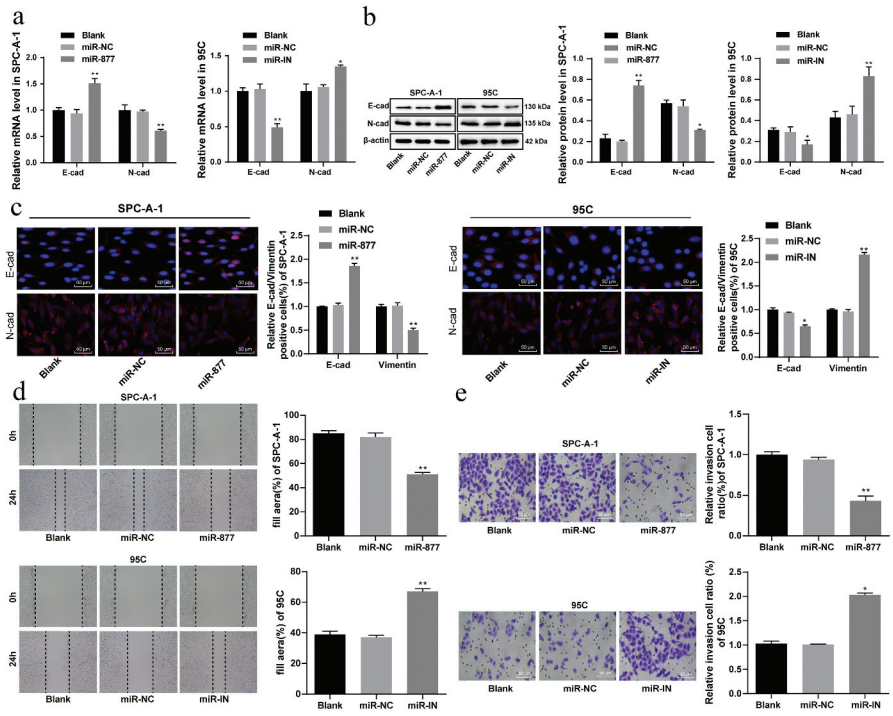

Figure 5. Overexpression of miR-877 inhibits the EMT, cell migration and invasion of LC cells. In the SPC-A-1 cells miR-877 was overexpressed and in the 95 C cells the miR-877 was inhibited. (a). Relative mRNA expression of EMT markers; (b). Relative protein levels of EMT markers; (c). Relative E-cadherin positive cells and decreased vimentin in SPC-A-1 cells and 95 C cells by immunofluorescence assay; (d). Relative migration ability of SPC-A-1 cells and 95 C cells *in vitro*; (e). Relative invasive ability of SPC-A-1 cells and 95 C cells *in vitro*. The experiment was performed three times independently. The results are presented as the mean ± standard deviation. Compared to the miR-NC group, * $p < 0.05$, ** $p < 0.01$. miR-877, microRNA-877; LC, lung cancer; EMT, Epithelial-mesenchymal transition; NC, negative control.

Compared with that in the NC group, cell viability in the OE group was significantly higher (Figure 6 (ce)), the proportion of cells in G2/M phase was evidently reduced, while the proportion of cells in S phase was enhanced (Figure 6(f)), and cell apoptosis was significantly lower (Figure 6(g,h)). E-cadherin levels in the OE group were remarkably lower, while N-cadherin levels were notably higher (Figure 6(i,j)). The numbers of E-cadherin-positive cells decreased and vimentin positive cells increased in the OE group relative to the NC group (Figure 6(k)). The migration (Figure 6(l)) and invasion (Figure 6(m)) of SPC-A-1 cells in the OE group also increased noticeably (all $p < 0.05$).

miR-877 inactivates PI3K/AKT pathway by decreasing ACP5

A literature review indicated that ACP5 could promote the progression of colon cancer and liver cancer by activating the PI3K/AKT pathway. Therefore, we detected the protein level and phosphorylation level of PI3K and AKT in SPC-A-1 cells and PC5 cells by western blot analysis. The results showed no significant difference in the levels of total AKT and total PI3K between the miR-877 and NC groups ($p > 0.05$); while the phosphorylation levels of AKT and PI3K were significantly decreased in cells overexpressing miR-877. Cells overexpressing both ACP5 and miR-877 had restored phosphorylation levels of p-AKT and p-PI3K compared with cells overexpressing miR-877 alone (all $p < 0.05$). The phosphorylation levels of AKT and PI3K in 95 C cells in the miR-IN group were notably higher than those in the miR-NC group (both $p < 0.05$, Figure 7). Combining the above results, we concluded that miR-877 inhibited NSCLC cell growth by targeting ACP5 and inactivating the PI3K/AKT pathway.

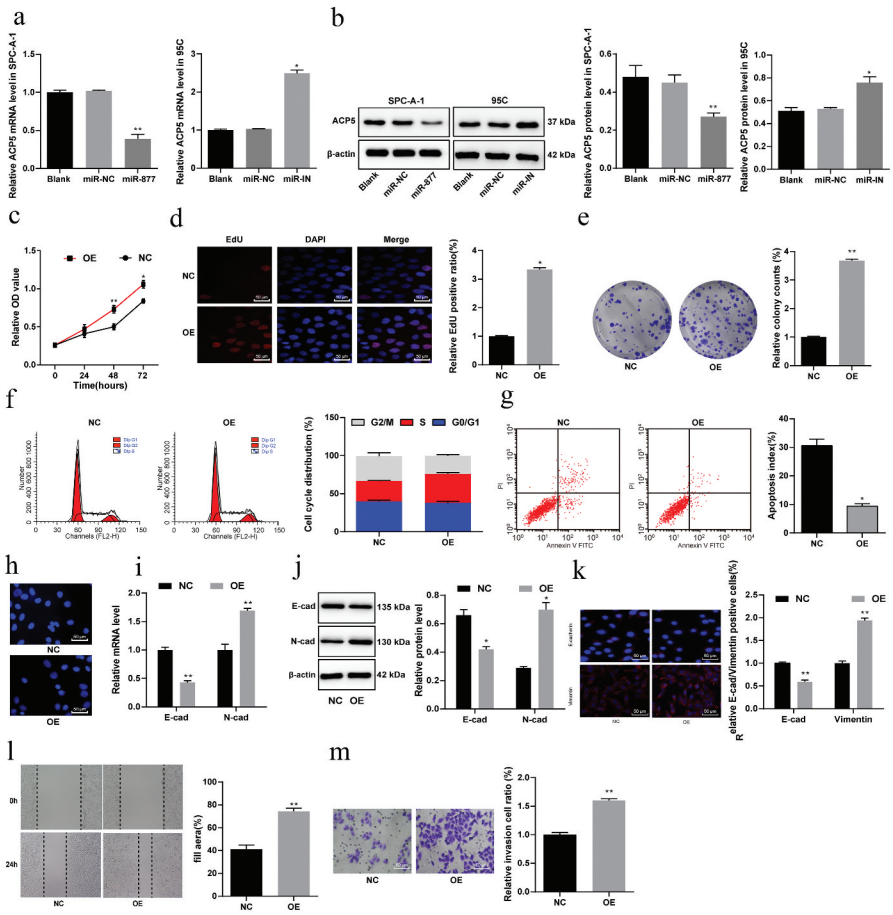

Figure 6. miR-877 suppresses the growth, invasion and migration of NSCLC cells by decreasing ACP5. (a). Relative mRNA expression of ACP5 in SPC-A-1 cells and 95 C cells measured by qRT-PCR; (b). Relative protein level of ACP5 in SPC-A-1 cells and 95 C cells detected by western blot analysis; (c). Relative OD value detected by MTT assay; (d). Relative EdU positive ratio detected by EdU assay; (e). Relative colony formation ability of cells determined by colony formation assay; (f). Relative cell cycle distribution detected by flow cytometry; (g). Relative apoptosis rate detected using flow cytometry; H. Representative images of apoptotic cells measured by Hoechst 33,258 staining; (i). Relative mRNA expression of E-cadherin and N-cadherin measured by qRT-PCR; (j). Relative protein levels of E-cadherin and N-cadherin detected by western blot analysis; (k). Representative images of E-cadherin positive cells decreased and vimentin-positive cells obtained by immunofluorescent staining; (l). Relative migration ability of cells determined by scratch test; (m). relative invasion ability of cells determined by Transwell assay. The experiment was performed three times independently. The results are presented as the mean ± standard deviation. Compared to the miR-NC group, * $p < 0.05$, ** $p < 0.01$. miR-877, microRNA-877; LC, lung cancer; ACP5, tartrate resistant acid phosphatase 5; OD, optical density; EdU, 5-ethynyl-2 -deoxyuridine; NC, negative control.

Overexpression of miR-877 inhibits growth of xenograft tumor *in vivo*

The effect of miR-877 on SPC-A-1 and PC5 cell growth *in vivo* was evaluated by calculating the volume and weight of xenograft tumors. Compared with that in mice in the miR-NC group, the tumor volume in the miR-877 group decreased noticeably, while in the miR-IN group, the tumor volume increased (both $p < 0.05$, Figure 8(a)). The detection on weight and volume of tumors after mice were fed for 5 weeks were also consistent with this observation ($p < 0.05$, Figure 8(b)).

Ki67 is a proliferating cell-related nuclear antigen, the function of which is closely related to mitosis and is indispensable in cell proliferation. In the clinic, the malignant degree of cancer can be judged by the positive rate of Ki67 in tumor cells. Compared with that in the miR-NC group, the positive rate of Ki67 in the miR-877 group decreased significantly but increased in the miR-IN group (both $p < 0.05$, Figure 8(c)). These

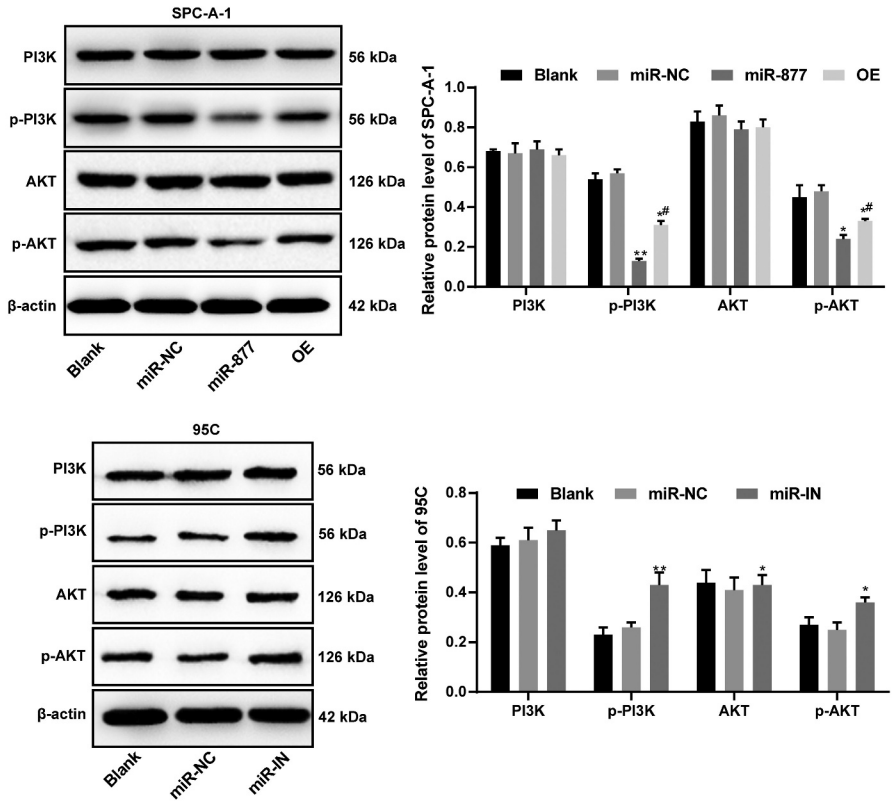

Figure 7. miR-877 inhibits NSCLC cell growth by targeting ACP5 and inactivating the PI3K/AKT pathway. The experiment was performed three times independently. The results are presented as the mean ± standard deviation. Compared to the miR-NC group, * $p < 0.05$, ** $p < 0.01$; compared to the miR-877 group, # $p < 0.05$. miR-877, microRNA-877; LC, lung cancer; ACP5, tartrate resistant acid phosphatase 5; PI3K, phosphatidylinositol-3 kinase; AKT, protein kinase B; NC, negative control.

results indicated that overexpression of miR-877 inhibited SPC-A-1 cell proliferation.

TUNEL staining results of mouse xenograft tumors revealed that the TUNEL-positive rate in mice tumors in the miR-877 group was noticeably higher but was greatly lower than that in the miR-IN group (both $p < 0.05$) (Figure 8(d)).

Discussion

As LC is the most frequently diagnosed and fatal human cancers, LC patients have an extremely poor prognosis with a very low 5-year survival rate due to the lack of recognized markers in the early stage [16]. Although novel molecular targeted treatment methods have achieved satisfactory efficacy in some cancer types, no targeted therapeutic approach can be applied to most LC patients so far [17]. miRs have been commonly recognized to exert crucial functions in regulating EMT and biological processes of NSCLC cells [18]. In this study, we hypothesized that miR-877 may play a role in LC cell growth and EMT through the involvement of ACP5 and the PI3K/AKT pathway. Consequently, our findings revealed that overexpression of miR-877 inhibited NSCLC cell growth and EMT by downregulating ACP5 and inactivating the PI3K/AKT pathway.

The first major finding was that miR-877 was poorly expressed in LC tissues and cells. miR-877 expression is also downregulated in the plasma and tissues of patients with RCC, and might be an underlying marker for the diagnosis and prognosis of RCC [10]. Additionally, we confirmed that miR-877 expression was related to the clinical stage, differentiation degree, lymph node metastasis and prognosis of LC patients, which further supported the association of miR-877 expression with LC progression. Similarly, the abnormal low expression of miRs has been previously reported to

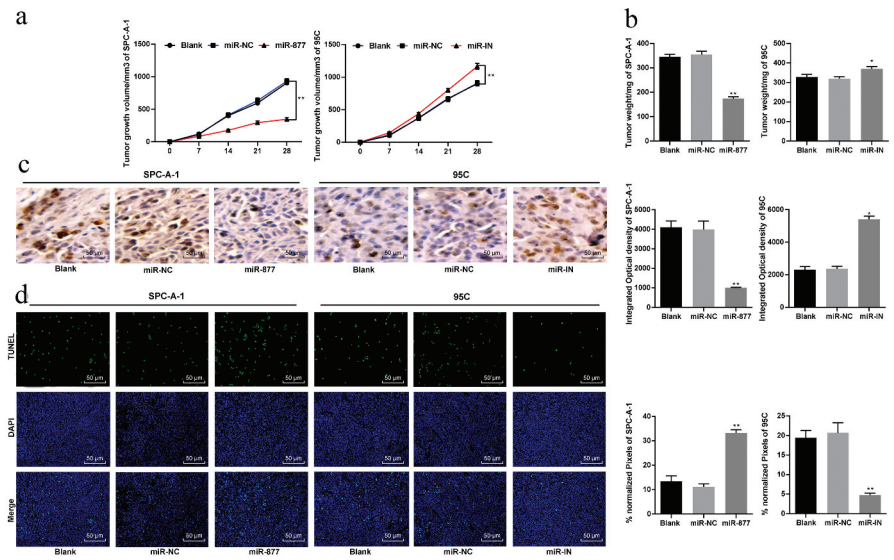

Figure 8. Overexpression of miR-877 inhibits LC cell growth *in vivo*. (a). Relative tumor volume in each group; (b). Relative tumor weight in each group; (c). Relative positive rate of Ki67 in tumor cells by immunohistochemistry; (d). Representative images of TUNEL-positive rate in mouse tumors. Compared to the miR-NC group, * $p < 0.05$, ** $p < 0.01$, n = 5. miR-877, microRNA-877; LC, lung cancer; NC, negative control.

be associated with the pathological characteristics of LC patients. Luo and his colleagues reported that miR-449a expression was obviously reduced in LC tissues and that its downregulation was closely associated with advanced pathological staging, lymph node metastasis and poor survival in NSCLC patients [19].

Moreover, our data confirmed that overexpressed miR-877 induced apoptosis and cell cycle arrest and inhibited the EMT, migration and invasion of NSCLC cells. Consistent observation of miR-877 inhibition of cell proliferation and viability has been found in hepatocellular carcinoma, demonstrating the protective roles of miR-877 in malignant tumors [20]. Our study further supported that miR-877 could promote cell apoptosis, as evidenced by the upregulation of cleaved caspase-3 and cleaved PARP, along with the downregulation of Bcl-xl. Bcl-xl, a critical apoptosis inhibitor, is always overexpressed in NSCLC, contributing to inhibited apoptosis and undesirable prognosis and thus plays a key role in tumor progression [21]. Caspase-3 is a key effector protease that is cleaved and activated during apoptosis, which in turn cleaves PARP, whose cleavage is an effective biomarker of apoptosis [22]. A study suggested that downregulation of caspase-3 is related to lymph node metastasis, poor prognosis and chemotherapy resistance of NSCLC [23]. You *et al.* found that overexpressed miR-449a induced LC cell cycle arrest, promoted cell apoptosis and suppressed cell growth [24], which was in agreement with our results. Additionally, E-cadherin and vimentin are considered as main biomarkers of EMT and E-cadherin expression is commonly lost in the process of EMT [25]. Loss of E-cadherin has been associated with promoted invasive capacity and high tumor grade and poor prognosis [26]. Yun *et al.* indicated that NSCLC cells achieve stronger migration and invasion abilities, stem cell like features and drug resistance through EMT [27], the primary step of LC metastasis in SPC-A1 cells [28]. A recent study revealed a similar result that the overexpression of miR-30a enhanced E-cadherin expression but reduced the expression of N-cadherin and vimentin [29]. Interestingly, restoration of miR-33b expression inhibited lung adenocarcinoma cell proliferation, migration, and invasion and EMT *in vitro* [30], which is in line with our results.

Furthermore, a dual-luciferase reporter gene assay verified that miR-877 could target ACP5 to negatively regulate its expression. As previously reported, ACP5 was upregulated in lung adenocarcinoma tissues, and its overexpression showed a strong link with lymph node metastasis and differentiation [13]. Additionally, we found that miR-877 blocked the activation of the PI3K/AKT pathway in NSCLC cells by targeting ACP5. Guerriero I *et al.* confirmed that overactivation of the PI3K/AKT pathway was observed in NSCLC, which contributed to the occurrence and development of cancer and increased the resistance to chemotherapy and radiotherapy against NSCLC [31]. Similarly, overexpression of miR-126 inhibited EMT and LC cell metastasis by inactivating the PI3K/AKT/Snail axis [28].

Overall, our study supported that miR-877 overexpression repressed NSCLC cell growth by targeting ACP5 and inhibiting the PI3K/AKT pathway. These results indeed demonstrated a novel approach for NSCLC treatment. The exact mechanism of miR-877 in NSCLC with regards to the involvement of ACP5 and the PI3K/AKT pathway should be studied in more detail clearly in the future. Although our findings offer therapeutic implications for NSCLC treatment, the experimental results and effective application in clinical practice require further validation.

Disclosure statement

The authors declare no conflicts of interest.

References

[1] Santos FN, De Castria TB, Cruz MR, et al. Chemotherapy for advanced non-small cell lung cancer in the elderly population. Cochrane Database Syst Rev. 2015;10:CD010463.

[2] Bach PB, Mirkin JN, Oliver TK, et al. Benefits and harms of CT screening for lung cancer: a systematic review. JAMA. 2012;307(22):2418–2429. .

[3] Mulherkar R, Grewal AS, Berman AT. Emerging role of immunotherapy in locally advanced non-small cell lung cancer. Clin Adv Hematol Oncol. 2020;18 (4):212–217.

[4] Reck M, Popat S, Reinmuth N, et al. Metastatic non-small-cell lung cancer (NSCLC): ESMO clinical practice guidelines for diagnosis, treatment and follow-up. Ann Oncol. 2014;25(Suppl 3):iii27–39. .

[5] Fajersztajn L, Veras M, Barrozo LV, et al. Air pollution: a potentially modifiable risk factor for lung cancer. Nat Rev Cancer. 2013;13(9):674–678. .

[6] Torres-Duran M, Fernandez-Villar A, Barros-Dios JM, et al. Residential radon: the neglected risk factor in lung cancer risk scores. J Thorac Oncol. 2016;11 (9):1384–1386. .

[7] Zarogoulidis P, Baka S, Labaki S, et al. Targeted lung cancer treatments and eye metastasis. Med Hypothesis Discov Innov Ophthalmol. 2017;6(1):10–13.

[8] Yao Z, Fenoglio S, Gao DC, et al. TGF-beta IL-6 axis mediates selective and adaptive mechanisms of resistance to molecular targeted therapy in lung cancer. Proc Natl Acad Sci U S A. 2010;107 (35):15535–15540. .

[9] Shen J, Liao J, Guarnera MA, et al. Analysis of MicroRNAs in sputum to improve computed tomography for lung cancer diagnosis. J Thorac Oncol. 2014;9 (1):33–40. .

[10] Shi Q, Xu X, Liu Q, et al. MicroRNA-877 acts as a tumor suppressor by directly targeting eEF2K in renal cell carcinoma. Oncol Lett. 2016;11 (2):1474–1480. .

[11] Wang C, Gu S, Cao H, et al. miR-877-3p targets Smad7 and is associated with myofibroblast differentiation and bleomycin-induced lung fibrosis. Sci Rep. 2016;6 (30122).

[12] Halling Linder C, Ek-Rylander B, Krumpel M, et al. Bone alkaline phosphatase and tartrate-resistant acid phosphatase: potential co-regulators of bone mineralization. Calcif Tissue Int. 2017;101(1):92–101. .

[13] Gao YL, Liu MR, Yang SX, et al. Prognostic significance of ACP5 expression in patients with lung adenocarcinoma. Clin Respir J. 2018;12(3):1100–1105. .

[14] Chen M, Du Y, Qui M, et al. Ophiopogonin B-induced autophagy in non-small cell lung cancer cells via inhibition of the PI3K/Akt signaling pathway. Oncol Rep. 2013;29(2):430–436.

[15] Ji Y, Han Z, Shao L, et al. Evaluation of in vivo antitumor effects of low-frequency ultrasound-mediated miRNA-133a microbubble delivery in breast cancer. Cancer Med. 2016;5(9):2534–2543. .

[16] Torre LA, Siegel RL, Jemal A. Lung cancer statistics. Adv Exp Med Biol. 2016;893(1–19).

[17] Li C, Lyu J, Meng QH. MiR-93 promotes tumorigenesis and metastasis of non-small cell lung cancer cells by activating the PI3K/Akt pathway via inhibition of LKB1/PTEN/CDKN1A. J Cancer. 2017;8(5):870–879.

[18] Ke Y, Zhao W, Xiong J, et al. miR-149 inhibits non-small-cell lung cancer cells EMT by targeting FOXM1. Biochem Res Int. 2013;2013:506731.

[19] Luo W, Huang B, Li Z, et al. MicroRNA-449a is down-regulated in non-small cell lung cancer and inhibits migration and invasion by targeting c-Met. PLoS One. 2013;8(5):e64759. .

[20] Huang X, Qin J, Lu S. Up-regulation of miR-877 induced by paclitaxel inhibits hepatocellular carcinoma cell proliferation though targeting FOXM1. Int J Clin Exp Pathol. 2015;8(2):1515–1524.

[21] Othman N, In LL, Harikrishna JA, et al. Bcl-xL silencing induces alterations in hsa-miR-608 expression and subsequent cell death in A549 and SK-LU1 human lung adenocarcinoma cells. PLoS One. 2013;8(12):e81735. .

[22] Xu P, Cai X, Zhang W, et al. Flavonoids of Rosa roxburghii Tratt exhibit radioprotection and anti-apoptosis properties via the Bcl-2(Ca(2+))/Caspase-3/PARP-1 pathway. Apoptosis. 2016;21(10):1125–1143. .

[23] Cui R, Kim T, Fassan M, et al. MicroRNA-224 is implicated in lung cancer pathogenesis through targeting caspase-3 and caspase-7. Oncotarget. 2015;6(26):21802–21815. .

[24] You J, Zhang Y, Liu B, et al. MicroRNA-449a inhibits cell growth in lung cancer and regulates long noncoding RNA nuclear enriched abundant transcript 1. Indian J Cancer. 2014;51(Suppl 3):e77–81. .

[25] Yamashita N, Tokunaga E, Iimori M, et al. Epithelial Paradox: clinical Significance of Coexpression of E-cadherin and Vimentin With Regard to Invasion and Metastasis of Breast Cancer. Clin Breast Cancer. 2018;18(5):e1003–e1009. .

[26] Myong NH. Loss of E-cadherin and acquisition of vimentin in epithelial-mesenchymal transition are noble indicators of uterine cervix cancer progression. Korean J Pathol. 2012;46(4):341–348.

[27] Yuan X, Wu H, Han N, et al. Notch signaling and EMT in non-small cell lung cancer: biological significance and therapeutic application. J Hematol Oncol. 2014;7:87.

[28] Jia Z, Zhang Y, Xu Q, et al. miR-126 suppresses epithelial-to-mesenchymal transition and metastasis by targeting PI3K/AKT/Snail signaling of lung cancer cells. Oncol Lett. 2018;15(5):7369–7375.

[29] Wang X, Qiu H, Tang R, et al. miR30a inhibits epithelialmesenchymal transition and metastasis in triplenegative breast cancer by targeting ROR1. Oncol Rep. 2018;39(6):2635–2643.

[30] Qu J, Li M, An J, et al. MicroRNA-33b inhibits lung adenocarcinoma cell growth, invasion, and epithelial-mesenchymal transition by suppressing Wnt/beta-catenin/ZEB1 signaling. Int J Oncol. 2015;47(6):2141–2152.

[31] Guerriero I, D'angelo D, Pallante P, et al. Analysis of miRNA profiles identified miR-196a as a crucial mediator of aberrant PI3K/AKT signaling in lung cancer cells. Oncotarget. 2017;8(12):19172–19191.